

INSTITUTE FOR NUCLEAR STUDY  
UNIVERSITY OF TOKYO  
Tanashi, Tokyo 188  
Japan

## Nuclear Structure of $^{17}\text{Ne}$ by the Three-neutron Pick-up ( $^3\text{He}, ^6\text{He}$ ) Reaction

V. GUIMARÃES, S. KUBONO, N. IKEDA, I. KATAYAMA,  
T. NOMURA, M. H. TANAKA, Y. FUCHI, H. KAWASHIMA

Institute for Nuclear Study, University of Tokyo,  
3-2-1 Midori-cho, Tanashi, Tokyo, 188 Japan.

S. KATO

Physics Department, Yamagata University, Yamagata, 990 Japan.

H. TOYOKAWA

Physics Department, University of Tsukuba, Tsukuba, 305 Japan.

C. C. YUN, T. NIIZEKI

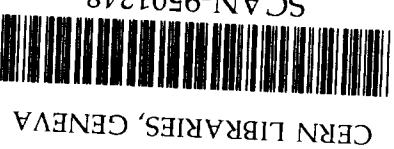
Physics Department, Tokyo Inst. of Technology, Meguro, Tokyo, 152 Japan.

T. KUBO, M. OHURA

Institute of Physical and Chemical Research (RIKEN)  
2-1 Hirosawa, Wako, Saitama, 351-01 Japan.

M. HOSAKA

Physics Department, Tohoku University, Aoba, Sendai, 980 Japan.



SW 3506

# Nuclear Structure of $^{17}\text{Ne}$ by the Three-Neutron Pick-up ( $^3\text{He}, ^6\text{He}$ ) Reaction

V. Guimarães, S. Kubono, N. Ikeda, I. Katayama, T. Nomura,  
M. H. Tanaka, Y. Fuchi, H. Kawashima, S. Kato <sup>a</sup>, H. Toyokawa <sup>b</sup>,  
C. C. Yun <sup>c</sup>, T. Niizeki <sup>c</sup>, T. Kubo <sup>d</sup>, M. Ohura <sup>d</sup> and M. Hosaka <sup>e</sup>

*Institute for Nuclear Study, University of Tokyo,*

*3-2-1 Midori-cho, Tanashi, Tokyo, 188 Japan*

<sup>a</sup> *Physics Department, Yamagata University, Yamagata, 990 Japan*

<sup>b</sup> *Physics Department, University of Tsukuba, Tsukuba, 305 Japan*

<sup>c</sup> *Tokyo Institute of Technology, Meguro, Tokyo, 152 Japan*

<sup>d</sup> *Institute of Physical and Chemical Research (RIKEN)*

*2-1 Hirosawa, Wako, Saitama, 351-01 Japan*

<sup>e</sup> *Physics Department, Tohoku University, Aoba, Sendai, 980 Japan*

January 5, 1995

---

## Abstract

The nuclear structure of  $^{17}\text{Ne}$  has been studied by the  $^{20}\text{Ne}(^3\text{He}, ^6\text{He})^{17}\text{Ne}$  reaction at 70 MeV. Fifteen levels were identified in  $\text{Ne}^{17}$ , and angular distributions have been measured for the first time for this reaction. The observed transferred angular momentum dependence of the angular distributions allowed spin-parity assignment. The  $T = \frac{3}{2}$  quartet analog states

in mass  $A = 17$  have been completed for six levels. The level shifts are analyzed in terms of the isobaric multiplet mass equation. The results show a slight linear dependence of the  $b$  and  $c$  coefficients of this equation on the excitation energy. The coefficients for the positive parity states seem to suggest different systematics from the negative parity states. The  $d$  coefficient has a large deviation from zero for the positive parity states, in particular for the  $\frac{5}{2}^+$  state, which could be indicating an extended radial wavefunction or some isospin symmetry breaking nuclear interaction effects.

keywords: NUCLEAR REACTION:  $^{20}\text{Ne}(^3\text{He}, ^6\text{He})^{17}\text{Ne}$ ,  $E_{\text{LAB}} = 70.079$  MeV; measured  $\sigma(\Theta)$ ,  $\Theta_{\text{LAB}} = 7^\circ$  to  $38^\circ$ ,  $^{17}\text{Ne}$  deduced mass excess, excitation energies,  $J, \pi$ ; IMME analysis of  $T = \frac{3}{2}$  quartet analog states in mass  $A = 17$ .

---

## 1 Introduction

The structure of nuclei near the drip lines is one of the major concerns in nuclear physics. Multi-nucleon transfer reactions have shown to be a powerful tool for studying nuclei near the drip lines in light mass region. These reactions allow to investigate exotic states such as high spin or many-particle many-hole states in these nuclei. In particular, the three-neutron pick-up ( $^3\text{He}, ^6\text{He}$ ) reaction has been used in the past mostly for precise mass measurements of proton-rich nuclei in the  $1p$  and  $2s-1d$  shell region [1-3]. However, the recently measured angular distributions of this reaction [4, 5] have shown a characteristics of transferred angular-momentum ( $L$ ) dependence, indicating that this reaction is a very useful spectroscopic tool to investigate these nuclei. Three-nucleon transfer reactions are experimentally difficult since the cross-sections involved are generally very small. Nevertheless, the development of a detector system including an accurate proportional gas counter [6] and a high-resolution magnetic spectrograph [7] has allowed measurements of extremely small cross-sections of such reactions.

We report here the experimental results and the analysis on the nuclear structure of  $^{17}\text{Ne}$  by this three-neutron transfer reaction. The properties of light nuclei with  $T_z = -\frac{3}{2}$

are usually known much less than those of their mirror nuclei. For the  $^{17}\text{Ne}$  nucleus the mass excess had been determined and a few low-lying excited states had been previously suggested [3, 8]. On the other hand, many  $T = \frac{3}{2}$  states of other three members ( $^{17}\text{N}$ ,  $^{17}\text{O}$  and  $^{17}\text{F}$ ) are known. Therefore, the quartet of analog state was determined before only for the ground and the first excited states in  $^{17}\text{Ne}$ . Thus, the determination of the level structure of  $^{17}\text{Ne}$  is specifically interesting as it permits an analysis in terms of the Isobaric Multiplet Mass Equation (IMME) for many states in a system. This is the first extensive study for quartets of several excited states in one multiplet system, and an analysis on these quartets can bring valuable spectroscopic information on the structure of  $A = 17$  nuclei.

The experimental setup and the procedure are described in Section 2, while the experimental results and the analysis in terms of DWBA are reported in Section 3. The interpretation of level scheme of  $^{17}\text{Ne}$  in terms of a large-base shell model is discussed in Section 4. The Section 5 is devoted to present an analysis in terms of the IMME, and where the level shift of several excited states is discussed. Finally, a summary is given in Section 6.

## 2 Experiment

The experiment was carried out with the sector-focusing cyclotron of the Institute for Nuclear Study, University of Tokyo. The incident energy of the  $^3\text{He}$  beam was 70.079-MeV and the average current obtained was about  $0.5 \mu\text{A}$ . The beam was transported into the scattering chamber, where a gas target system was mounted. The target system consisted of a gas cell and a  $^{24}\text{Mg}$  metallic foil of  $812 \pm 20 \mu\text{g}/\text{cm}^2$  thickness used for the energy calibration. The cell was filled with 99.95% isotopically enriched  $^{20}\text{Ne}$  gas to a pressure of 21 cm Hg. In the measurements with the gas target, a rectangular double-slit system was used, defining the solid angle 1 to 3 msr, depending on the detection angle.

The reaction products were momentum-analyzed by a QDD-type magnetic spectrograph [7] and detected by a hybrid-type gas proportional counter [6], especially designed

to minimize the background for low-event rate experiments. A thin plastic scintillator was set just behind the proportional counter for energy and time-of-flight measurements.

The particles were identified by using a set of signals, namely, energy, energy loss from the proportional counter and time-of-flight. The time-of-flight of the particles was obtained by the time interval between the cyclotron-RF and the fast signal from the plastic scintillator. The vertical position, perpendicular to the directions of momentum dispersion as well as to the particle trajectory, were also measured on the focal plane and used to reduce the background not arising from the target. Pile-up rejection was applied in order to reduce the background arising from the high counting rate of alpha particles.

The momentum spectra of  $^6\text{He}$  particles were measured at 12 angles between  $\Theta_{\text{LAB}} = 7.0^\circ$  and  $38.0^\circ$ . The spectrum at  $\Theta_{\text{LAB}} = 10^\circ$  was calibrated in energy by using the known states of  $^{21}\text{Mg}$  from the  $^{24}\text{Mg}(^3\text{He}, ^6\text{He})^{21}\text{Mg}$  reaction [5] in the same experimental run. Using this calibration, the momentum spectra of all other angles were converted to the energy spectrum and summed up. The total counts of each spectrum were normalized by multiplying the counts by the ratio of integrated charge, target thickness and solid angle at  $10.0^\circ$  and the values at the corresponding angle. The summed spectrum of  $\Theta_{\text{LAB}} = 7.0^\circ$  to  $29.0^\circ$  is presented in Fig. 1. The overall energy resolution achieved was about 180 keV FWHM, due mainly to the straggling in energy of the  $^6\text{He}$  particles in the gas target system. The spectra were analyzed by fitting the shape of the peaks with a Gaussian function with exponential tails, where the parameters were obtained from the fitting of the ground-state peak. The small peak around 3.300 MeV is due to a small peak appeared only in the spectra measured at  $\Theta_{\text{LAB}} = 22.0^\circ$  and  $25.0^\circ$ . Thus, it is not clear if it is a state in  $^{17}\text{Ne}$ .

The excitation energies and the uncertainties of the states observed in  $^{17}\text{Ne}$  are listed in Table 1. The uncertainties in the value of mass excess and excitation energies were determined by taking into account all the experimental accuracies such as the uncertainty in the absolute energy of the incident beam, the effective target thickness, and the energy loss of the particles in the gas target. The major errors come from the uncertainties in determining the peak positions in the fitting procedure. In particular, the state at 5.141 MeV has a large uncertainty because it was very close to the large  $^9\text{C}(\text{g.s.})$  contam-

ination peak. The present results on the excitation energies are in good agreement with, but much more accurate than the previously suggested values for  $^{17}\text{Ne}$  [8], which are listed in the last column in the table for comparison. The uncertainties on the experimental differential cross-sections were obtained by taking into account uncertainties, such as the statistical uncertainties in the yield and background of the peaks; and uncertainties in accumulated charge, target thickness and solid angle. The final values were estimated to be between 10% to 20%.

### 3 Experimental results and the DWBA analysis

The experimental angular distributions of  $^6\text{He}$  from the  $^{20}\text{Ne}(^3\text{He},^6\text{He})^{17}\text{Ne}$  reaction measured for 9 levels are shown in Figs. 2(a) - 2(e). In this figure the angular distributions are classified by their shapes, which are mainly determined by the transferred angular momenta ( $L$ ), as will be discussed later in this section. The measured differential cross-sections are generally small, being in the range of a few tens of nb/sr for the highly excited states. All the angular distributions show distinct behaviors at the forward angles, supporting the general feature of  $L$  dependence, as expected in direct multi-nucleon transfer reactions [9].

The analysis of the characteristic behavior at the forward angles in the angular distributions has been made in terms of the exact finite-range DWBA calculation, using the computer code TWOFNR [10]. Because both the target and ejectile nuclei have spin  $0^+$ , the transition has a single value for the transferred orbital angular momentum ( $L$ ) and two possible values for the transferred total angular momentum ( $J = L \pm \frac{1}{2}$ ). The transitions should also satisfy the energy conservation rule [9],

$$\sum(2n_i + l_i) = 2N_1 + L_1 + 2\nu + \lambda \quad \text{for the target system,} \quad (1)$$

$$\sum(2n_i + l_i) = 2N_2 + L_2 + 2\nu + \lambda \quad \text{for the ejectile system,} \quad (2)$$

where  $n_i$  and  $l_i$  are the number of radial nodes (excluding the origin) and the orbital angular momentum of each constituent nucleon in the shell model;  $N_i$  and  $L_i$  are those

of the 3n-cluster relative to the core, and  $\nu$  and  $\lambda$  are those of the internal motion in the 3n-cluster. Since a direct one-step process of a 3n-cluster transfer was assumed, the internal motion of the three identical fermions should have  $\nu = 0$  and  $\lambda = 1$ , which implies that the 3n-cluster should have  $J^\pi = \frac{3}{2}^-$  and  $L_2 = 1(N_2 = 0)$  for the motion with respect to the  $^3\text{He}$  core. Thus, for the low-lying states of the residual nucleus, the 3n-cluster should have  $L_1 = 1(N_1 = 1)$  for  $L = 0$  transitions, where  $\vec{L} = \vec{L}_1 + \vec{L}_2$ . For transitions with  $L = 1$  we have  $2N_1 + L_1 = 4$  for  $^{20}\text{Ne}$ , which gives two possibilities for the quantum numbers of the relative motion:  $L_1 = 2(N_1 = 1)$  or  $L_1 = 0(N_1 = 2)$ . These two possibilities for the quantum numbers did not change the positions of the maxima and minima in the calculated angular distributions, but, since they give small changes in the relative intensity of the maxima, the set that better reproduced the experimental angular distributions was chosen.

The optical potential parameters in Table 2, used in the calculations, were obtained from ref. [11], for the incident channel, while that for  $^6\text{He}$  was obtained from those of  $^6\text{Li}$  in ref. [12]. These parameter sets were also used in the analysis of angular distributions of the  $^{24}\text{Mg}(^3\text{He},^6\text{He})^{21}\text{Mg}$  reaction [5]. For the bound state parameters of the 3n-cluster, we adopted  $r_0 = 1.32 \text{ fm}$  and  $a = 0.65 \text{ fm}$  in  $^{20}\text{Ne}$ , and  $r_0 = 1.58 \text{ fm}$  and  $a = 0.65 \text{ fm}$  in  $^6\text{He}$ , where the radius was defined by  $R = r_0 \cdot A_{\text{core}}^{\frac{1}{3}}$ . These radius parameters are slightly larger than the value often used ( $r_0 = 1.25 \text{ fm}$ ). Although these radius parameters produced larger amplitudes of the oscillations in the angular distributions, they did not modify the general pattern. The potential depths were adjusted to reproduce the binding energies.

The calculated angular distributions are also shown in Figs. 2(a) - 2(e). The general shapes of the angular distributions at forward angles and the oscillations phases (maximum and minimum angles) are reasonably well reproduced by the calculations with the  $L$ -values denoted in the figures. These fits were obtained without modifying the optical potential parameters and the bound state potential parameters. The calculated angular distributions show a dominant role of  $L$ , i.e., there was little change in shape at forward angles for the total angular momentum transferred  $J = L \pm \frac{1}{2}$ . Thus,  $L$  is uniquely determined for each transition, but there are two choices of the spin of the residual nucleus,

J, for each L in assignment. The parity of the transition is given by  $\pi = (-1)^L$ .

The transferred angular momentum, the parity and the total angular momentum assigned for each state are summarized in Table 1. The ground state transition has  $L = 1$  as expected, since the spin  $J^\pi = \frac{1}{2}^-$  is known [13]. The angular distribution of the 1.908 MeV state has a clear  $L = 0$  shape, and thus  $J^\pi = \frac{1}{2}^+$  is uniquely assigned for this state. The states at 2.765 and 4.010 MeV have clearly  $L = 2$ . However, since there are two choices of J for each L, reasonable J's have been chosen by comparing with the corresponding levels in the mirror nucleus  $^{17}\text{N}$  [14, 15, 16]. Thus,  $J^\pi = \frac{5}{2}^+$  and  $J^\pi = \frac{3}{2}^+$  spins were assigned for the states at 2.765 and 4.010 MeV, respectively. The angular distributions of the 1.764, 2.623 and 3.043 MeV transitions have  $L = 3$  dependence. Moreover, the differential cross-section for the transition of 3.043 MeV decreases around  $10^\circ$  more than the prediction by the  $L = 3$  curve, indicating also a possibility of  $L = 0$ . See Fig. 2(d). Therefore this state at 3.043 MeV was assumed to be the analog of the 3.129 MeV state in  $^{17}\text{N}$ , and thus,  $J^\pi = \frac{7}{2}^-$  was assigned for it. The smooth variation in energy along the quartet of this state enforcing also the assignment. For the state at 1.764 MeV was assigned  $J^\pi = \frac{5}{2}^-$ . The ambiguity of  $J^\pi = \frac{5}{2}^-$  or  $J^\pi = \frac{7}{2}^-$  was left for the 2.623 MeV state, since there is no clear analog state in the mirror nucleus. The angular distribution of the 3.548 MeV state is fitted by  $L = 5$ . This state is considered to be the analog of the 3.629 MeV state in  $^{17}\text{N}$ , and  $J^\pi = \frac{9}{2}^-$  is assigned.

## 4 Comparison with shell model calculations

Shell model calculations performed for mass 17 nuclei [17-21] suggested the importance of particle-hole excitations for the structure of low-lying states in these nuclei. Most of the calculations were based on the weak coupling model [24], in which the correlation between particles in the same major shell is of predominant importance and the particle-hole interaction is treated as a small perturbation. The low-lying negative parity states in  $A = 17$  nuclei arise mainly from coupling of a  $p_{\frac{1}{2}}$  hole to positive parity states of mass 18. Besides these 2p-1h configurations, 4p-3h configurations are expected to play a role, while

the positive parity states are expected to be 3p-2h and 5p-4h. These works, however, differ in the shell model space or in the number of configurations taken into account, and even in the choice of the residual interactions, which, as pointed out by Margolis and Takacsy [17], could have a large influence on the energy spectrum.

We here compare the experimental levels in  $^{17}\text{Ne}$  with an extensive shell model calculation by Warburton and Millener [21]. Since their calculations do not include any Coulomb effect, they can be compared to the experimental energy levels in both  $^{17}\text{Ne}$  and  $^{17}\text{N}$  nuclei. They used a modified Millener-Kurath interaction (designated MK3) to describe the cross-shell interaction in which valence nucleons are active in several major shells simultaneously. This interaction is based on a multirange parametrization obtained by Hosaka et. al [22]. They defined the  $(0s)^4(0p)^{12}(1s0d)$  configuration as  $0\hbar\omega$ . The low-lying negative parity levels in  $^{17}\text{N}$  and  $^{17}\text{Ne}$  are predominantly from  $1\hbar\omega$ . The model space for the positive-parity states included all possible  $2\hbar\omega$  excitations as  $(0s)^3(0p)^{12}(1s0d)^2$  and  $(0s)^4(0p)^{11}(1s0d)^1(0f1p)^1$  configurations as well as the main  $(0s)^4(0p)^{10}(1s,0d)^3$  configurations. In Fig. 3, we show the energy level scheme of  $^{17}\text{Ne}$  compared with the  $2p - 1h$  and  $3p - 2h$  states predicted by this calculation. In the calculation the first ten odd-parity states are considered, according to the weak coupling model notation, to be mainly composed of,

$$\pi p_{\frac{1}{2}}^{-1} \otimes [^{18}\text{O}(0_1^+, 2_1^+, 4_1^+, 2_2^+, 0_3^+, 3_1^+)] \quad (3)$$

As may be seen in the figure there is a good one-to-one correspondence for the low-lying states in  $^{17}\text{Ne}$ , indicating that the main configuration of these states is well characterized by the weak coupling model assumed. Among the first ten states only the state at 3.713 MeV does not have a counterpart in the calculated spectra, and the state corresponding to the 2.623 MeV in  $^{17}\text{Ne}$  has too high energy in the calculated spectrum. The other disagreement are the predicted seconds  $\frac{1}{2}^-$  and  $\frac{3}{2}^-$  states, which do not have counterparts in the present  $^{17}\text{Ne}$  spectrum, since they were not clearly observed. These two states appear at 3.663 and 3.204 MeV in  $^{17}\text{N}$ , respectively. However, the 3.204 MeV state has a very small spectroscopic factor in the  $^{18}\text{O}(d,^3\text{He})^{17}\text{N}$  reaction [20], which corroborates with the small spectroscopic factor calculated by Warburton and Millener [21]. In terms

of the weak-coupling model these seconds  $\frac{1}{2}^-$  and  $\frac{3}{2}^-$  states would be formed by coupling a  $p$ -hole to the  $0_3^+$  and  $2_2^+$  states in  $A = 18$  nuclei, respectively. The low-lying positive states in  $A = 18$  nuclei have basically  $2p-0h$  configuration. However, to describe correctly the excitation energies and electromagnetic properties of the positive-parity levels in  $A = 18$ ,  $^{16}\text{O}$  core polarization have been considered in some shell model calculations [23-26]. This corresponds to allowing higher particle-hole excitations like  $4p-2h$  for the wave-functions of the positive-parity states. In particular, it was found in these shell model calculations that although the main configuration for  $0_3^+$  and  $2_2^+$  states in  $^{18}\text{Ne}$  and  $^{18}\text{O}$  is  $2p-0h$ , the  $4p-2h$  component of the wave-functions has a large amplitude. However, since the seconds  $\frac{1}{2}^-$  and  $\frac{3}{2}^-$  states in  $^{17}\text{Ne}$ , which are mainly  $2p-1h$  configuration, are not populated by the present  $3n$ -pickup reaction, one would expect that the two  $0_3^+$  and  $2_2^+$  parent states in  $A = 18$  are predominantly  $4p-2h$  states.

We may conclude this section by saying that the experimental  $^{17}\text{Ne}$  level scheme is overall in good agreement with the shell model calculation based on the weak coupling model, although the nuclear structure of these levels is not yet completely well understood.

## 5 The isobaric multiplet mass equation

From the present work the mass excess of  $^{17}\text{Ne}$  is determined to be  $16.453 \pm 0.032$  MeV. In Table 3 it is compared with other experimental values [3, 8] and with some theoretical and empirical predictions [27, 28]. The agreement with other measurements is good within the indicated errors. The evaluation by Wapstra et al. [28] is only an average of the two experimental results from references [3] and [8]. The isobaric multiplet mass equation (IMME) prediction for the mass excess of  $^{17}\text{Ne}$  was obtained with the coefficients for the ground-state (lowest  $\frac{1}{2}^-$ ) from Table 4 using only three other members of the isobaric analog state.

In Fig. 4, we plot all the firmly established experimental data on the  $T = \frac{3}{2}$  states of mass  $A = 17$ . In the case of  $^{17}\text{O}$  and  $^{17}\text{F}$ , we plot the energy difference ( $E - E_0$ ), where  $E$  stands for the excitation energy, and  $E_0 = 11.079$  MeV and  $11.193$  MeV are the lowest

$T = \frac{3}{2}$  states in  $^{17}\text{O}$  and  $^{17}\text{F}$ , respectively. Thus, the  $\frac{1}{2}^-$ ,  $\frac{3}{2}^-$ ,  $\frac{5}{2}^-$ ,  $\frac{1}{2}^+$ ,  $\frac{5}{2}^+$  and  $\frac{7}{2}^-$  quartets appear to be complete. For the low-lying states in  $^{17}\text{Ne}$ , only the quartet of the second  $\frac{3}{2}^-$  state was not completed, since this state is missing in the  $^{17}\text{Ne}$  spectrum, as pointed out in the previous section.

An analysis in terms of the IMME,

$$M(A, T_x) = a + b \times T_x + c \times T_x^2, \quad (4)$$

was made for these states. The parameters  $a$ ,  $b$  and  $c$  in Table 4 were obtained from the experimental values of the mass excess listed, using only the data from three members of the multiplet ( $^{17}\text{N}$ ,  $^{17}\text{O}$  and  $^{17}\text{F}$ ). The energies predicted for the states in  $^{17}\text{Ne}$  by the IMME are presented in the last column of Table 1. Except for the  $\frac{5}{2}^+$  level, to which the prediction gives 146 keV lower energy, all the other energies are in very good agreement with the observed excitation energies in  $^{17}\text{Ne}$  within the errors. The state at 3.043 MeV was assumed to be the fourth member of the  $\frac{7}{2}^-$  multiplet, although the state at 2.623 MeV also has  $J^\pi = (\frac{5}{2}^-, \frac{7}{2}^-)$  assignment.

Now, by using the mass excess of the four members of the multiplet, one can determine the coefficients of the IMME including the cubic term  $d \times T_x^3$ , which should, in principle, be zero if the isospin is a good quantum number. The coefficients obtained are listed in the second line for each state in Table 4. Apparently, inclusion of the  $^{17}\text{Ne}$  data, and consequently the  $d$  coefficient, does not change the  $a$ ,  $b$  and  $c$  significantly from the previous values. The exceptions, however, are the coefficients of the positive parity states  $\frac{1}{2}^+$  and  $\frac{5}{2}^+$ . The  $b$ ,  $c$  and  $d$  coefficients are plotted in Figs. 5(a) - 5(c) as a function of excitation energy in  $^{17}\text{Ne}$ . The  $b$  and  $c$  coefficients for the negative parity states have a weak linear dependence on excitation energy as:

$$\frac{\Delta b}{\Delta E_x} = +15 \text{ keV/MeV} \quad \text{and} \quad \frac{\Delta c}{\Delta E_x} = -7.5 \text{ keV/MeV}, \quad (5)$$

which are much smaller than the prediction for  $A = 17$  by Skwiersky et al. [29]. In their analysis only the energies of the ground and first excited states in  $^{17}\text{Ne}$  were used, and the ordering of the  $\frac{7}{2}^-$  and  $\frac{3}{2}^-$  states in  $^{17}\text{O}$  were interchanged erroneously. Thus, their predictions gave quite different results, +42 keV/MeV and -18 keV/MeV for the  $b$  and

$c$  coefficient, respectively, as a function of excitation energy in  $^{17}\text{N}$ . The systematics of the  $b$  coefficient for the negative parity states is opposite to the  $A$  dependence, which is  $b(A) \approx -0.2A$  for  $A \leq 40$  [30]. The  $c$  coefficient has an oscillatory dependence on  $A$ , while the systematics obtained here show a slight linear dependence as a function of excitation energy for negative parity states. One can also see clearly that the coefficients of the positive parity states do not follow the systematics for the negative parity states.

The  $b$  and  $c$  coefficients are very different quantities and they can be understood by examining their origin or nature. According to Jänecke [31], the masses of the members of an isobaric multiplet are given by:

$$M(A, T, T_z) = \frac{1}{2}(m_n + m_H)A + \Delta_{nH}T_z + \langle \alpha TT_z | H_0 | \alpha TT_z \rangle + \langle \alpha TT_z | H_C^{(k)} | \alpha TT_z \rangle, \quad (6)$$

where  $H_0$  is the charge-independent part of the nuclear Hamiltonian, and  $H_C^{(k)}$  is the charge dependent interactions, mainly Coulomb interaction, between the protons in the nucleus, and  $\Delta_{nH}$  is the neutron-hydrogen mass difference, 0.782339(17) MeV. If we treat the Coulomb interaction as a perturbative term in the total Hamiltonian, and neglect the isospin dependent nuclear interaction, then to first order we have:

$$\langle \alpha TT_z | H_C^{(k)} | \alpha TT_z \rangle = E_C^{(0)}(A, T) - E_C^{(1)}(A, T)T_z + [3T_z^2 - T(T-1)]E_C^{(2)}(A, T), \quad (7)$$

where  $E_C^{(0)}$ ,  $E_C^{(1)}$  and  $E_C^{(2)}$  are the scalar, vector and tensor Coulomb energies, respectively. The coefficients of the IMME are related to these energies by:

$$a(A, T) = \frac{1}{2}(m_n + m_H)A + \langle \alpha TT_z | H_0 | \alpha TT_z \rangle + E_C^{(0)}(A, T) - T(T+1)E_C^{(2)}(A, T) \quad (9)$$

$$b(A, T) = \Delta_{nH} - E_C^{(1)}(A, T) \quad (9)$$

$$c(A, T) = 3E_C^{(2)}(A, T) \quad (10)$$

Now, the Coulomb displacement or Coulomb shift  $\Delta E_C$  between any two members of the isobaric multiplet is given by:

$$\Delta E_C(A, T, T_z - k | T_z) = k[E_C^{(1)}(A, T) - \Delta_{nH}] - 3k(2T_z - k)E_C^{(2)}(A, T) \quad (11)$$

with integer  $k$  and  $|T_z| \leq T$  and  $|T_z - T| \leq k$ , and  $\Delta_{nH}$  stands for the difference in proton and neutron mass.

For analog states in conjugate nuclei one obtains:

$$\Delta E_C(A, \frac{3}{2}, -\frac{3}{2} | +\frac{3}{2}) = 3[E_C^{(1)}(A, \frac{3}{2}) - \Delta_{nH}] = -3b \quad (12)$$

and between  $T_z = \frac{1}{2}$  and  $\frac{3}{2}$  members:

$$\Delta E_C(A, \frac{3}{2}, +\frac{1}{2} | +\frac{3}{2}) = [E_C^{(1)}(A, \frac{3}{2}) - \Delta_{nH}] - 3[2E_C^{(2)}(A, \frac{3}{2})] = -b - 2c \quad (13)$$

Thus, the coefficients  $b$  and  $c$  of the IMME, which are experimentally obtained, can be compared with the vector and tensor parts of the charge dependent interaction (mainly Coulomb interaction), which may be obtained theoretically.

In the absence of Coulomb interaction and if nuclear force is charge symmetric, the coefficients  $b$  and  $c$  would be zero, and the level displacement would vanish. As a consequence, the spectra of mirror nuclei would be identical. However, due to the charge dependent interaction corresponding levels are shifted in the mirror pairs, and excited states often deviate by tens or sometimes even a few hundreds of keV in addition to the ground states shift. In the present case the positive and negative parity states in the mirror nuclei have a different sign of shift relative to the ground states. In other words, the excitation energies of negative parity states in  $^{17}\text{Ne}$  are lower than those of the analogs in  $^{17}\text{N}$ , while the excitation energies of positive parity states are opposite. The absolute level shift for the positive parity states are also larger than for the negative parity states. Since data on excited state isobaric multiplets of  $T = \frac{3}{2}$  are quite limited for light nuclei, excited state multiplets have received less attention than the ground state multiplets in the theoretical point of view. However, an extensive calculation of level displacement energy was made by de Meijer [32]. He used, in his calculation, different wave functions for protons and neutrons in a large shell model base. The results of this ambitious calculation for the first two negative and positive parity states in  $^{17}\text{Ne}$  are presented in Table

5. The calculation gives larger level displacement energies for the negative parity states and smaller ones for the positive parity states. The difference of the calculated values from the experimental ones may be attributed to the fact that they used a fixed set of parameters for the Woods-Saxon potential for a large mass region,  $A = 9-28$ . The level displacement energy is very sensitive to a small change in the radius parameter  $r_0$ ; for  $\Delta r_0 = 0.01 \text{ fm}$  one finds  $\Delta E \approx 30 \text{ keV}$  for instance.

Besides above considerations, Bertsch [33] has shown that two-particles correlation in the Coulomb interaction plays a very important role to explain the state dependence of Coulomb energies for the  $0^+$ ,  $2^+$  and  $4^+$  excited states pairs in  $^{18}\text{O}$ - $^{18}\text{Ne}$  doublet. If the  $2p-1h$  configurations in  $^{17}\text{Ne}$  are formed by coupling a neutron-hole to the excited states of  $^{18}\text{Ne}$ , as discussed in Section 4, this correlation may be important to describe correctly the Coulomb energies in the  $A = 17$  nuclei.

The  $d$  coefficient obtained for the negative parity states are consistent with zero. However the  $d$  coefficient derived for one of the two positive parity states ( $\frac{5}{2}^+$ ) has a significant deviation from zero. See Fig. 5(c). This term is given by:

$$d = \frac{1}{6} \times \{M(\frac{3}{2}) - M(-\frac{3}{2}) - 3 \times [M(\frac{1}{2}) - M(-\frac{1}{2})]\}, \quad (14)$$

where  $M(T_z)$  is the mass excess of the nucleus with  $T_z$ . As is clear from the equation, the  $d$  coefficient is three times more sensitive to the mass difference between the  $T_z = \pm \frac{1}{2}$  members of the multiplets than to that between the  $T_z = \pm \frac{3}{2}$  members. A non zero  $d$ , i.e., a deviation from the standard IMME (up to  $c$  coefficient), implies that the terms higher than the second order perturbation corrections of the Coulomb interaction or charge-symmetry breaking nuclear interactions should be considered. The  $d$  coefficient was obtained for twenty-two isobaric quartets [34]. It was found that they are consistent with zero, being the upper limit of their absolute values around 7 keV. An exception is the  $d$  coefficient for  $A = 9$  quartet  $d = 5.2 \pm 1.7 \text{ keV}$ , which is one of the best determined  $d$  coefficients. The value for the  $\frac{5}{2}^+$  positive-parity state of the present work is  $d = -17.0 \pm 6.9 \text{ keV}$ , which is very large if one compares with the systematics in ref. [34]. If there were a peak between the two states at 2.765 and 3.043 MeV, the excitation energy of the  $\frac{5}{2}^+$  state would be reduced to some extent, although there was no indication of another state there at any

angles measured. If one assumed a peak between them, the excitation energy estimated for the  $\frac{5}{2}^+$  state would be reduced at most 40 keV. This would bring  $d \approx -10.0$  for this level, which is still significantly large.

In an attempt to explain the deviation for mass  $A = 9$ , Auerbach and Lev [35] considered the isospin-mixing of  $T = \frac{1}{2}$  with  $T = \frac{3}{2}$  states, which can also produce a non zero  $d$  coefficient. The contribution due to the isospin-mixing was estimated to be only  $d \approx 1 \text{ keV}$  for very light nuclei and  $d \approx 3 \text{ keV}$  for  $A = 40$ . However, since the level density in the region of the lowest  $T = \frac{3}{2}$  states in  $^{17}\text{O}$  and  $^{17}\text{F}$  nuclei is smaller, about 7 to 10 levels/MeV, than in the similar excitation energy region in mass  $A = 40$ , one would expect contribution of at most 3 keV due to the isospin-mixing for  $A = 17$ . Bertsch and Kahana [36] estimated that the contribution of the second order term of the Coulomb interaction, which could be expressed in terms of a three-body force, was in the order of 1 keV for  $A = 9$  and less than 1 keV for heavier nuclei. Another possible effect is the radial extension of the wave function due to Coulomb effects. Since the neutrons in the neutron-rich members are converted to protons in the analog states, the Coulomb repulsion energy increases, and the nucleus would extend to some degree. This expansion is expected to be large for the  $s_{\frac{1}{2}}$  proton, since the potential has no centrifugal barrier. A calculation of this effect in  $A = 27$  [37] showed that the expansion of the wave-function caused a 110 keV change in the Coulomb energy of  $^{27}\text{P}$ , but it was absorbed by the other coefficients and did not produce any significant contribution to the  $d$  coefficient. However, the situation might change if the nucleons are largely unbound. This could be the case for the present  $\frac{5}{2}^+$  state, which is unbound by 1123 keV, while the  $\frac{1}{2}^+$  state is unbound only by 408 keV. It can be very interesting to understand the large  $d$  term investigating such possible extended structure by using reliable shell model calculations. Another possibility for the  $d$ -value could be due to the second order term of the isospin symmetry breaking nuclear interaction. This should be another interesting subject to be studied.



## 6 Summary

The  $^{20}\text{Ne}(^3\text{He}, ^6\text{He})^{17}\text{Ne}$  reaction has been investigated. It appears that this reaction proceeds predominantly through a direct three-neutron transfer mechanism. Fifteen levels were identified in  $^{17}\text{Ne}$  and the angular distributions for nine of them were measured. The clear transferred orbital angular momentum dependence observed in the angular distributions enabled spin parity assignment for the levels.

An analysis in terms of the isobaric multiplet mass equation up to  $d \times T_i^3$  term has been made for the first six states. Excitation energy dependence of these coefficients, including the cubic term  $d$  in the IMME, was observed. The different systematics of the  $b$  coefficients observed for the positive and negative parity states seem to be related to the shell model configurations expected for these states. The considerable deviation of the  $d$  coefficient from zero for the  $\frac{5}{2}^+$  state suggests a possible radial extension of the wavefunction well above the proton threshold or the effect of an isospin symmetry breaking nuclear interaction.

Isospin quartets well above the threshold were not studied before. Detailed theoretical analysis in terms of the IMME for the present  $A = 17$  system will be very interesting. More detailed shell model calculations with more suitable configurations and extraction of the matter radius and charge radius of the states in  $^{17}\text{Ne}$ , may aid in understanding the difference in the level displacement of the positive and negative parity states. Moreover, it seems that a detailed comparison between the experimental and calculated coefficients of the quadratic and cubic terms of IMME can bring important information about charge-dependent or isospin symmetry breaking nuclear interaction.

The authors are grateful to the cyclotron crew of the Institute for Nuclear Study. The authors are also grateful to Dr. S. Nakamura for discussions on the IMME coefficients systematics. One of the author (V.G.) was financially supported by the CNPq (Conselho Nacional de Pesquisa e Desenvolvimento)-Brasil and Inoue Foundation for Science in Japan and he is also indebted to RIKEN for providing him an accommodation while he was in Japan. All the DWBA calculations were made at FACOM computer of the INS.

## References

- [1] E. Kashy, W. Benenson, I. D. Proctor, P. Hauge, and G. Bertsch, *Phys. Rev. C* **7** (1973) 2251, and references therein.
- [2] G. F. Trentelman, B. M. Preedom, and E. Kashy, *Phys. Rev. Lett.* **25** (1970) 530.
- [3] R. Mendelson, G. J. Wozniak, A. D. Bacher, J. M. Cerny, *Phys. Rev. Lett.* **25** (1970) 533.
- [4] S. Kubono, N. Ikeda, T. Nomura, Y. Fuchi, H. Kawashima, S. Kato, H. Miyatake, and H. Orihara, *Phys. Rev. C* **4** (1991) 1821.
- [5] S. Kubono, Y. Funatsu, N. Ikeda, M. Yasue, T. Nomura, Y. Fuchi, H. Kawashima, S. Kato, H. Miyatake, H. Orihara and T. Kajino, *Nucl. Phys. A* **537** (1992) 153.
- [6] M. H. Tanaka, S. Kubono, and S. Kato, *Nucl. Instr. and Meth.* **195** (1982) 509.
- [7] S. Kato, M. H. Tanaka, and T. Hasegawa, *Nucl. Instr. and Meth.* **154** (1978) 19.
- [8] G. J. Wozniak, R. Mendelson, J. M. Loiseaux, J. Cerny, *Lawrence Berkeley Laboratory report LBL-1666* (1972) 76.
- [9] A. Arima and S. Kubono, *Treatise on Heavy-Ion Science*, Vol. 1, ed. D. A. Bromley, (Plenum, 1984) ch. 6.
- [10] M. Igarashi, unpublished (Institute for Nuclear Study, Univ. of Tokyo, 1991).
- [11] C. M. Perey and F. G. Perey, *Nucl. Data Table* **10** (1972) 539.
- [12] R. L. Kozub, et. al., *Phys. Rev. C* **27** (1983) 158.
- [13] J. C. Hardy, J. E. Esterl, R. G. Sextro and J. Cerny, *Phys. Rev. C* **3** (1971) 700.
- [14] Ajzenberg-Selove and references therein, *Nucl. Phys. A* **460** (1986) 1.
- [15] R. Jahn, D. P. Stahel, G. J. Wozniak, R. J. de Meijer and J. Cerny, *Phys. Rev. C* **18** (1978) 9.

- [16] G. E. Moore, M. E. Cobern, H. T. Fortune, S. Mordechai, R. V. Kollarits R. Middleton, *Phys. Lett.* **76B** (1978)192.
- [17] B. Margolis and N. de Takacsy, *Can. Jour. Phys.* **44** (1966) 1431.
- [18] B. S. Reehal and B. H. Wildenthal, *Part. Nucl.* **5** (1973) 137.
- [19] W. D. M. Rae, N. S. Godwin, D. Sinclair, H. S. Bradlow, P. S. Fisher, J. D. King, A. A. Pilt and G. Proudford, *Nucl. Phys.* **A319** (1979) 239.
- [20] G. Mairle, G. J. Wagner, K. T. Knoffe, Liu Ken Pao, H. Riedesel, V. Bechtold and L. Friedrich, *Nucl. Phys.* **A363** (1981) 413.
- [21] E. K. Warburton and D. J. Millener, *Phys. Rev.* **C39** (1989) 1120.
- [22] A. Hosaka, K. I. Kubo and H. Toki, *Nucl. Phys.* **A444** (1985) 76.
- [23] A. V. Nero, E. G. Adelberger and F. S. Dietrich, *Phys. Rev.* **C24** (1981) 1864.
- [24] P. S. Ellis and T. Engeland, *Nucl. Phys.* **A144** (1970) 161.
- [25] J. B. McGrory and B. H. Wildenthal, *Phys. Rev.* **C7** (1973) 974.
- [26] A. P. Zuker, *Phys. Rev. Lett.* **23** (1969) 983.
- [27] K. Gul, *J. Phys. Soc. Japan* **44** (1978) 353.
- [28] A. H. Wapstra, J. Britz and Pape, *Atomic Data and Nuclear Tables* **39** (1988) 281.
- [29] B. M. Skwiersky, C. M. Baglin and P. D. Parker, *Phys. Rev.* **C9** (1974) 910.
- [30] M. S. Antony, J. Britz, J. B. Bueb, and A. Pape, *Atomic data and Nuclear data Tables*, **33** (1985) 447.
- [31] J. Jänecke, *Isospin in Nuclear Physics*, ed. D. H. Wilkinson, (North-Holland, Amsterdam, 1969), chap. 8.
- [32] R. J. de Meijer, H. F. J. van Royen and Brussaard, *Nucl. Phys.* **A164** (1971) 11.
- [33] G. F. Bertsch, *Phys. Rev.* **174** (1968) 1313.

- [34] W. Benenson and E. Kashy, *Rev. Mod. Phys.* **51** (1979) 527.
- [35] N. Auerbach and A. Lev, *Nucl. Phys.* **A180** (1972) 651.
- [36] G.F. Bertsch and S. Kahana, *Phys. Lett* **33B** (1970) 193.
- [37] W. Benenson, D. Mueller, E. Kashy, H. Nann and L. W. Robinson, *Phys. Rev.* **C15** (1977) 1187.

## Figure Captions:

**Figure 1:** The summed  ${}^6\text{He}$  energy spectrum from the  ${}^{20}\text{Ne}({}^3\text{He}, {}^6\text{He}){}^{17}\text{Ne}$  reaction. The excitation energies in  ${}^{17}\text{Ne}$  are denoted.

**Figure 2:** Angular distributions of  ${}^6\text{He}$  from the  ${}^{20}\text{Ne}({}^3\text{He}, {}^6\text{He}){}^{17}\text{Ne}$  reaction for the states denoted, attributed to the transferred angular momenta: (a)  $L = 0$ ; (b)  $L = 1$ ; (c)  $L = 2$ ; (d)  $L = 3$  and (e)  $L = 5$ . The solid lines are the DWBA calculations for  $L_s$ ' indicated. See the discussion in text. Some angular distributions were multiplied by the factors indicated.

**Figure 3:** Energy levels of  ${}^{17}\text{Ne}$ . The theoretical predictions are taken from ref. [21]. The  $2p - 1h$  and  $3p - 2h$  model spectra are discussed in the text.

**Figure 4:**  $T = \frac{3}{2}$  energy levels in  $A = 17$  quartet. Excitation energies and  $J^\pi$  assignments are obtained from the compilation in ref. [14] for the  ${}^{17}\text{O}$  and  ${}^{17}\text{F}$ , from refs. [14,15] for  ${}^{17}\text{N}$ , and the results of the present experiment, for  ${}^{17}\text{Ne}$ . The lowest  $T = \frac{3}{2}$  state in  ${}^{17}\text{O}$ ,  ${}^{17}\text{F}$  and  ${}^{17}\text{N}$  were normalized to the ground state of  ${}^{17}\text{Ne}$ .

**Figure 5:** The coefficients of the IMME as a function of excitation energy in  ${}^{17}\text{Ne}$ ; (a) the  $b$  coefficient, (b) the  $c$  coefficient and (c) the  $d$  coefficient.

Table 1: Nuclear levels in  $^{17}\text{Ne}$  identified. The accuracies in parenthesis are in keV.

Ex. energy (MeV)	$\pm\Delta\text{Ex}$ (keV)	Transferred L	adopted $J^\pi$	Ex. <sup>b),c)</sup> (MeV)	Ex. <sup>d)</sup> (MeV)
0.0		1	$\frac{1}{2}^-$ <sup>a)</sup>		
1.288	8	1	$\frac{3}{2}^-$	1.35 (70)	1.284 (26)
1.764	8	3	$\frac{5}{2}^-$	1.84 (70)	1.754 (27)
1.908	8	0	$\frac{1}{2}^+$		1.916 (28)
2.623	9	3	$(\frac{5}{2}, \frac{7}{2})^-$		
2.765	12	2	$\frac{5}{2}^+$	2.77 (70)	2.619 (28)
3.043	11	3(0)	$\frac{7}{2}^-(\frac{1}{2}^+)$		3.006 (28)
3.548	20	5	$\frac{9}{2}^-$		
3.713	30				
4.010	10	2	$\frac{3}{2}^+$		
4.487	22				
5.141	62			5.28 (90)	
5.722	23				
6.132	35				
6.366	22				

a) From ref. [13].

b) From ref. [8].

c) The experimental errors in parentheses are in keV.

d) Predictions by the IMME using the coefficients from Table 4.

Table 2: Optical and binding potential parameters.

set	$V$ (MeV)	$r_R$ (fm)	$a_R$ (fm)	$W_V$ <sup>b)</sup> (MeV)	$r_I$ (fm)	$a_I$ (fm)	$r_C$ (fm)
$^3\text{He} + ^{20}\text{Ne}$	160.00	1.633	0.375	35.00	1.015	1.767	1.3
$^6\text{He} + ^{17}\text{Ne}$	64.70	1.250	0.717	13.00	1.250	0.800	1.3
$3n + ^{17}\text{Ne}$	a)	1.32	0.65				
$3n + ^3\text{He}$	a)	1.58	0.65				

a) The depth was adjusted to reproduce the binding energy.

b) The imaginary potential is a volume type Woods-Saxon potential for both systems.

Table 3: Comparison of the measurements and predictions of mass excess of  $^{17}\text{Ne}$ .

Authors	Mass excess (MeV)	ref.
<b>Experiment</b>		
Present	$16.453 \pm 0.032$	
Woznick et. al.	$16.480 \pm 0.050$	a)
Mendelson et. al.	$16.479 \pm 0.050$	b)
<b>Predictions</b>		
IMME	$16.496 \pm 0.018$	c)
Wapstra	$16.480 \pm 0.050$	d)
Jänecke-Masson	16.62	d)
Tachibana et al.	15.99	d)
Comay-Kelson-Zidon	16.92	d)
Pape-Antony	$16.73 \pm 0.33$	d)
Jänecke-Garvey-Kelson	16.630	d)
Gul	16.630	e)

a) ref. [8].

b) ref. [3].

c) Coefficients used in the IMME are listed in Table 4.

d) ref. [28].

e) ref. [27].

Table 4: Mass excesses (in MeV) and the coefficients of IMME for the  $T = \frac{3}{2}$  quartet of  $A = 17$ . The numbers in parenthesis are the errors in keV.

$J^\pi$	$^{17}\text{N}$	$^{17}\text{O}$	$^{17}\text{F}$	$^{17}\text{Ne}$	$a$ (MeV)	$b$ (MeV)	$c$ (MeV)	$d$ (keV)
	$(T_z = \frac{3}{2})$	$(T_z = \frac{1}{2})$	$(T_z = -\frac{1}{2})$	$(T_z = -\frac{3}{2})$				
$\frac{1}{2}^-$	7.871(15)	10.270(1)	13.145(2)	16.453(32)	11.648(2)	-2.875(2)	0.238(8)	
					11.651(3)	-2.877(3)	0.227(9)	7.2(6.0)
$\frac{3}{2}^-$	9.245(15)	11.657(1)	14.502(2)	17.741(33)	13.025(2)	-2.845(2)	0.217(8)	
					13.028(3)	-2.847(3)	0.207(9)	6.5(6.1)
$\frac{1}{2}^+$	9.721(15)	12.135(5)	15.032(5)	18.361(33)	13.527(5)	-2.897(6)	0.241(9)	
					13.526(5)	-2.899(8)	0.229(9)	8.5(7.0)
$\frac{5}{2}^-$	9.778(15)	12.189(1)	15.013(5)	18.217(33)	13.549(3)	-2.824(4)	0.207(8)	
					13.551(3)	-2.825(6)	0.198(9)	5.5(6.6)
$\frac{5}{2}^+$	10.397(15)	12.827(3)	15.733(5)	19.218(34)	14.220(3)	-2.906(5)	0.238(8)	
					14.214(4)	-2.902(7)	0.264(9)	-17.0(6.9)
$\frac{7}{2}^-$	11.000(15)	13.422(2)	16.256(4)	19.496(34)	14.788(3)	-2.834(4)	0.206(8)	
					14.788(3)	-2.834(4)	0.205(9)	1.0(6.6)

Table 5: Comparison of the experimental level displacement energies between  $^{17}\text{F}$  and  $^{17}\text{Ne}$  analog states, and excitation energies in  $^{17}\text{Ne}$  by the calculation [32]. The numbers in parenthesis are the errors in keV.

State	$\Delta E(exp)$ (MeV)	$\Delta E(calc)$ (MeV)	$\Delta E(exp) - \Delta E(calc)$ (keV)	Ex(exp) (MeV)	Ex(calc) (MeV)	Ex(exp)- Ex(calc) (keV)
$\frac{1}{2}^-$	4.090 (32)	4.245	-155	0	0	0
$\frac{3}{2}^-$	4.021 (33)	4.182	-161	1.288(8)	1.289	1
$\frac{1}{2}^+$	4.111 (33)	4.053	+ 58	1.908(8)	1.667	+241
$\frac{5}{2}^+$	4.266 (34)	4.154	+112	2.765(8)	2.486	+279

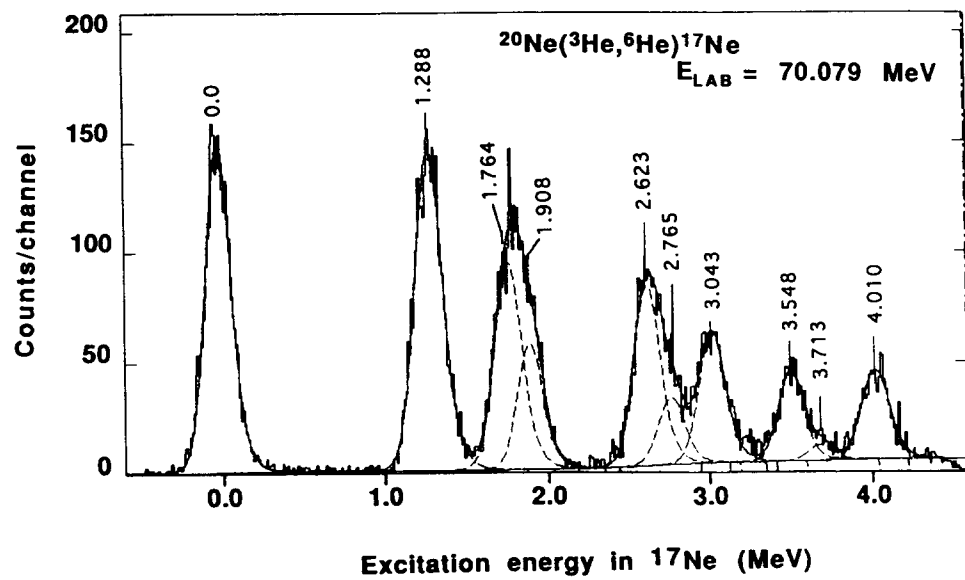


Figure 1

Figure 2 (a)

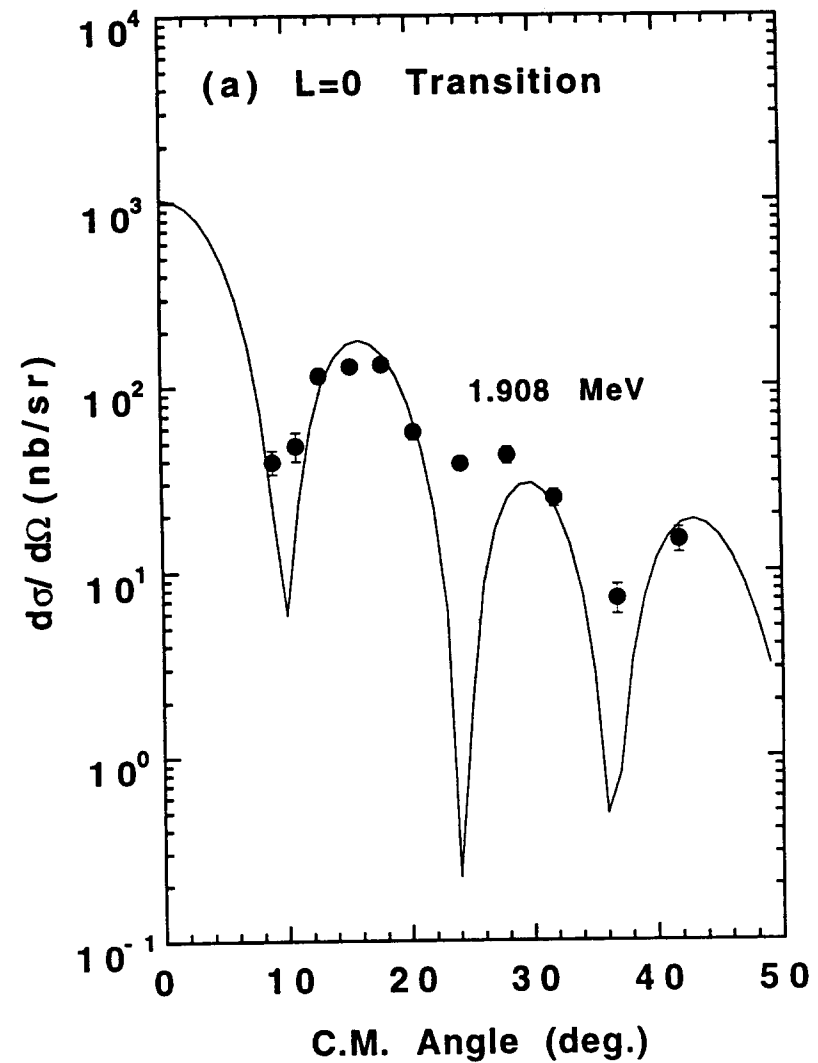


Figure 2 (b)

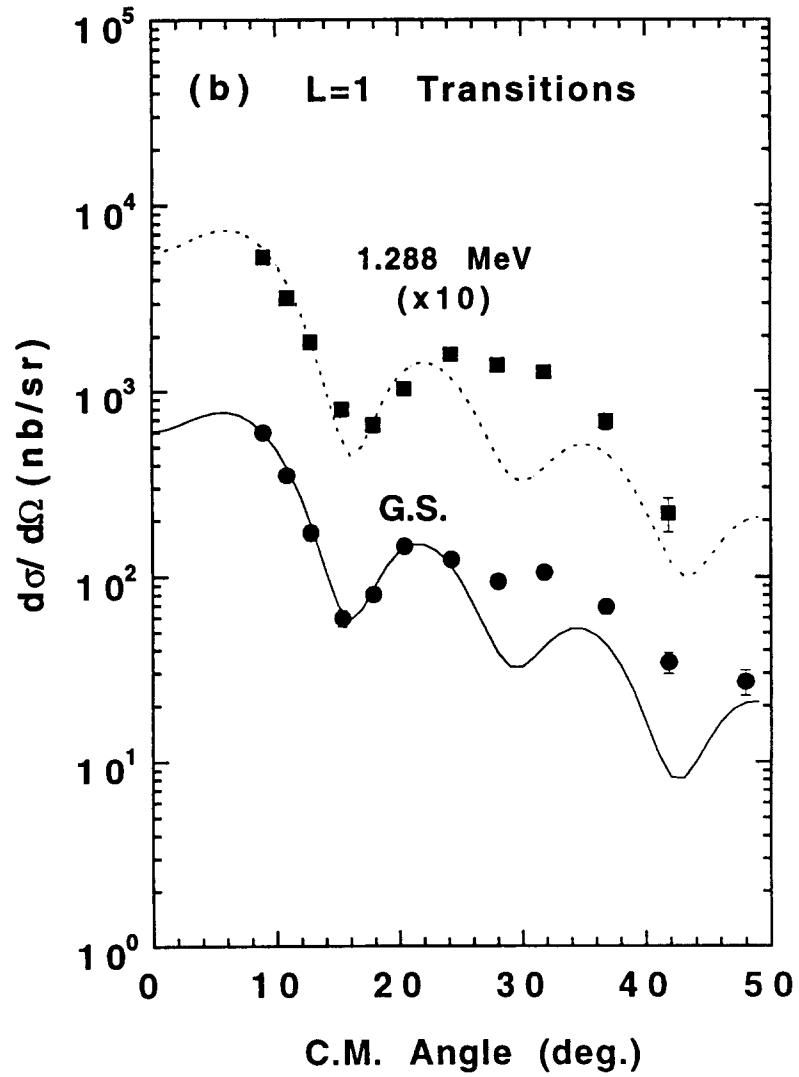


Figure 2 (c)

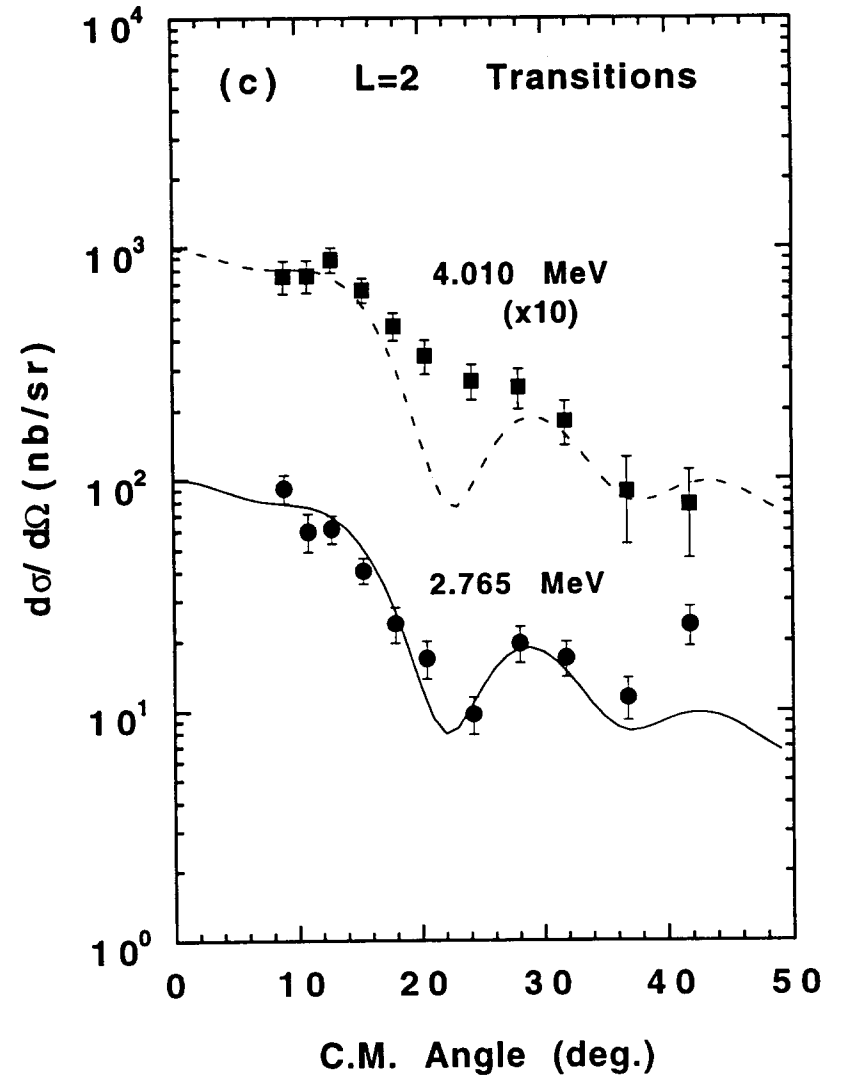


Figure 2 (d)

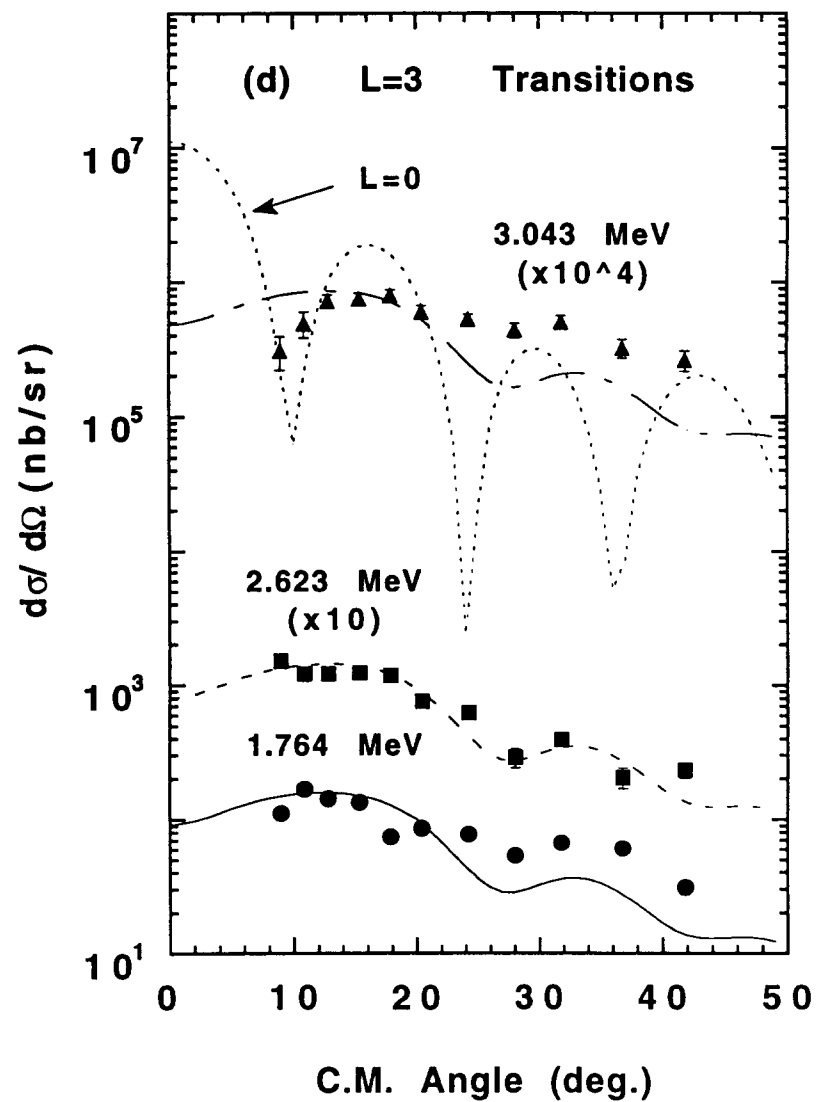
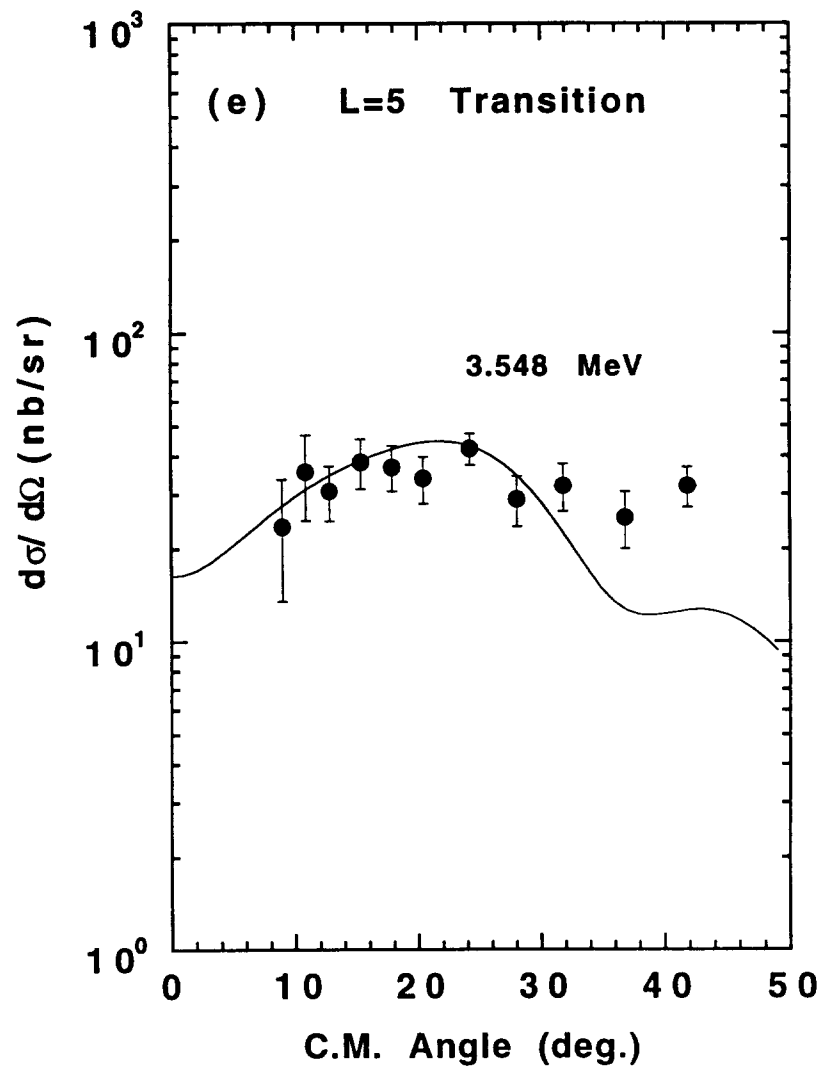


Figure 2 (e)



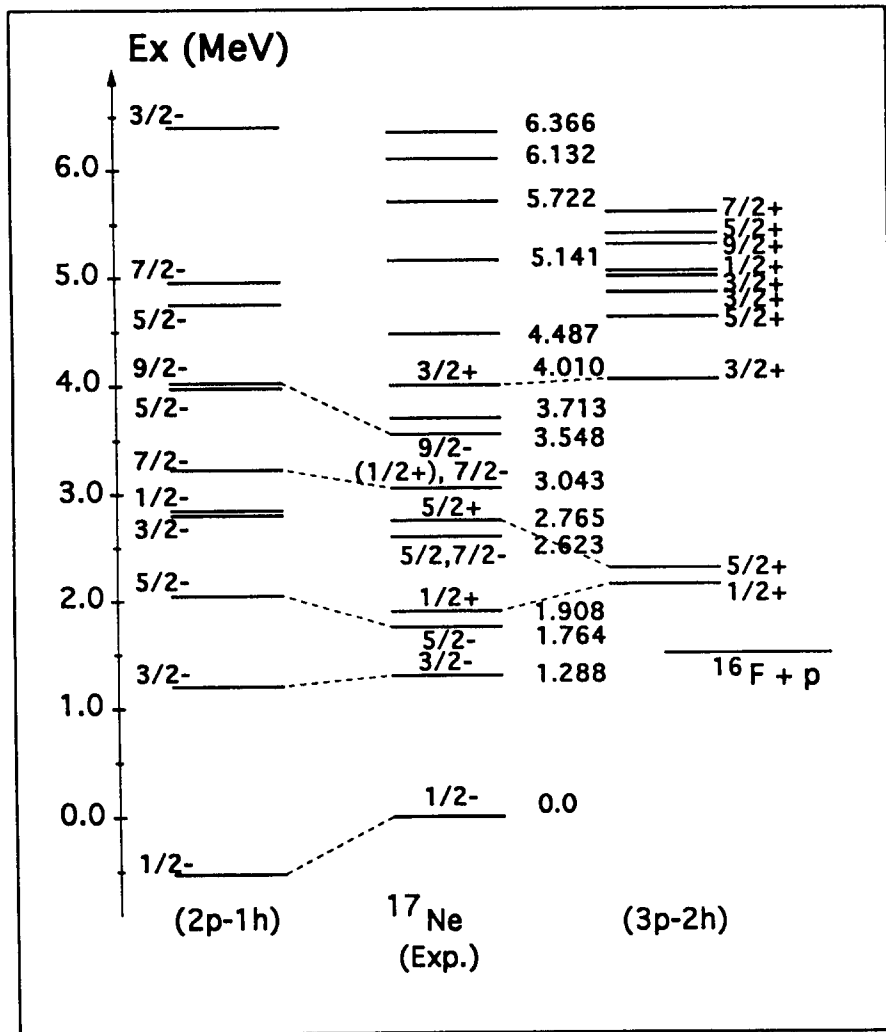


Figure 3

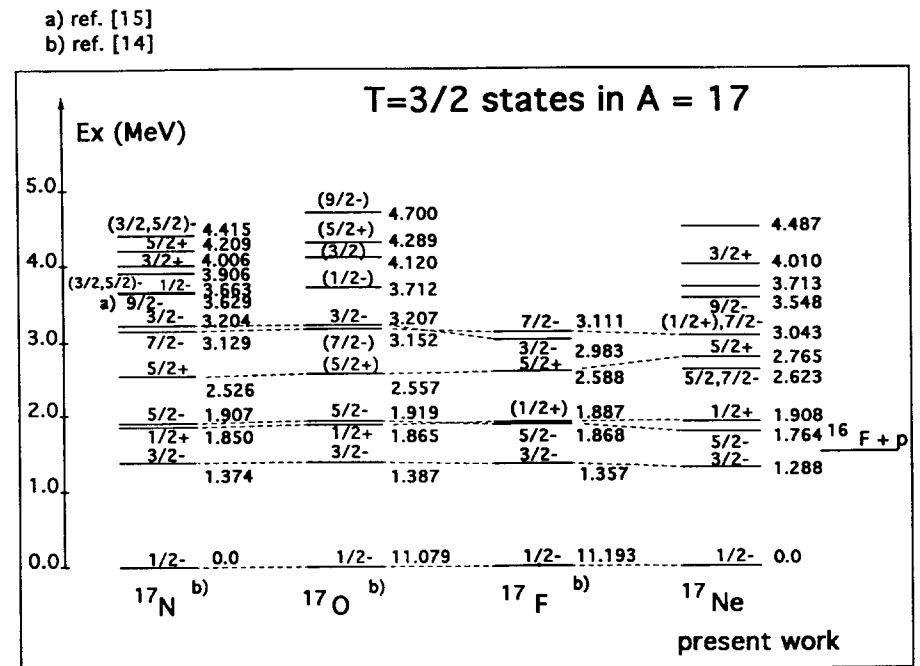


Figure 4



Figure 5

